Influence of Mg-doped barriers on semipolar (20$\bar{2}$1) multiple-quantum-well green light-emitting diodes

Chia-Yen Huang,[1,a)] Qimin Yan,[1] Yuji Zhao,[2] Kenji Fujito,[3] Daniel Feezell,[1]
Chris G. Van de Walle,[1] James S. Speck,[1] Steven P. DenBaars,[1,2] and Shuji Nakamura[1,2]
[1]*Department of Materials, University of California, Santa Barbara, California 93106, USA*
[2]*Department of Electrical and Computer Engineering, University of California, Santa Barbara, California 93106, USA*
[3]*Optoelectronics Laboratory, Mitsubishi Chemical Corporation, 1000 Higashi-mamiana, Ushiku, Ibaraki 300-1295, Japan*

(Received 31 July 2011; accepted 15 September 2011; published online 7 October 2011)

We report the effects of Mg doping in the barriers of semipolar (20$\bar{2}$1) multiple-quantum-well light-emitting diodes (LEDs) with long emission wavelengths (>500 nm). With moderate Mg doping concentrations (3×10^{18}–5×10^{18} cm^{-3}) in the barriers, the output power was enhanced compared to those with undoped barriers, which suggests that hole transport in the active region is a limiting factor for device performance. Improved hole injection due to Mg doping in the barriers is demonstrated by dichromatic LED experiments and band diagram simulations. With Mg-doped AlGaN barriers, double-quantum-well LEDs with orange to red emission ($\lambda > 600$ nm) were also demonstrated. © *2011 American Institute of Physics*. [doi:10.1063/1.3647560]

Recently, nitride-based light-emitting diodes (LEDs) and laser diodes (LDs) grown on nonpolar and semipolar bulk GaN substrates have been widely studied experimentally and theoretically.[1–9] Compared to conventional devices grown on c-plane, devices on nonpolar and semipolar planes are expected to have higher internal efficiency due to eliminated or reduced internal polarization.[1–5] Previously, efficient high power blue and green LEDs were demonstrated on the (10$\bar{1}$1) and the (11$\bar{2}$2) planes with three to six quantum wells (QWs) in the active region.[6,7] For yellow-green to yellow emission ($\lambda = 550$–580 nm), single-quantum-well (SQW) LEDs have been demonstrated on the (20$\bar{2}$1) and (11$\bar{2}$2) planes.[8,9] However, multiple-quantum-well (MQW) LEDs with long emission wavelengths (>500 nm) and output powers comparable to those of SQW LEDs have not been demonstrated on the (20$\bar{2}$1) plane. It has been reported that holes mostly populate the top QW nearest to the p-side, and the resulting uneven hole distribution is expected to reduce the overall recombination rate for c-plane LEDs.[10] As a potential solution, Han *et al*. demonstrated that Mg doping in the barriers enhanced the output power for blue MQW LEDs grown on c-plane due to improved hole injection efficiency.[11] In this paper, we report the effects of Mg doping in the barriers on (20$\bar{2}$1) double-quantum-well (DQW) LEDs with emission wavelengths in the green region and beyond.

DQW LEDs with undoped or Mg-doped middle barriers were grown by metalorganic chemical vapor deposition (MOCVD) on free-standing (20$\bar{2}$1) GaN substrates which were manufactured by Mitsubishi Chemical Corporation. The QWs were grown at 750 °C under atmospheric pressure. The thicknesses of the QWs and the barriers were estimated to be 3 nm and 10 nm, respectively. Five LEDs were grown with bis-cyclopentadienyl magnesium (Cp_2Mg) flow rates in the middle barrier of 0 (undoped), 0.6, 1, 3, and 5 sccm. Secondary ion mass spectroscopy (SIMS) confirmed the Mg concentration in the barrier to be 6×10^{18} cm^{-3} with the introduction of 1 sccm of Cp_2Mg during barrier growth. The background Mg concentration in the QWs was measured to be around one tenth of the Mg concentration in barrier, which can be attributed to Mg diffusion or the "memory effect" of the Cp_2Mg precursor in the reactor chamber. A linear relationship between Cp_2Mg flow rate and Mg concentration in the barriers and QWs is assumed in this work. After growth of the active region, a 10 nm p-$Al_{0.2}Ga_{0.8}N$ electron blocking layer (EBL) was deposited, followed by a 100 nm p-GaN capping layer. The size of the LED is 490×292 μm^2 (0.1 mm^2 injection area).

Figure 1(a) shows the forward voltages under 20 mA injection for the series of five LEDs. Although the forward voltages are relatively high, a clear reduction in voltage was observed when Mg doping was introduced into the middle barrier of the DQW LEDs. This result suggests the existence of carrier transport issues between QWs for long-wavelength (20$\bar{2}$1) MQW LEDs. The output powers of the LEDs with

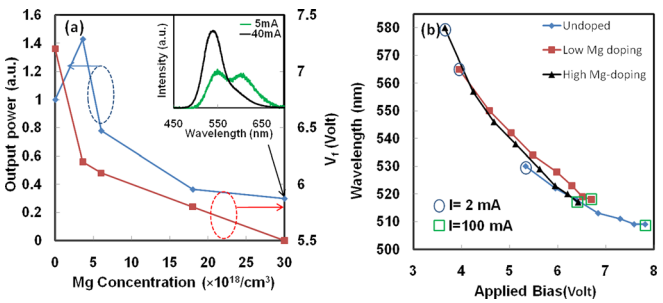

FIG. 1. (Color online) (a) Relative output power and forward voltage (V_f) under 20 mA injection for LEDs with different Mg doping levels in the barriers. The upper right corner shows the EL spectra under 5 mA and 40 mA injection for LEDs with high Mg doping levels (b) EL peak wavelength versus applied bias for current injection levels ranging from 2 mA to 100 mA for undoped, low-doped (3.6×10^{18} cm^{-3}), and high-doped (1.8×10^{19} cm^{-3}) barriers.

a)Electronic mail: chiayen@umail.ucsb.edu.

Mg-doped barriers relative to those with undoped barriers under the same injection current (I = 20 mA) are also shown in Figure 1(a). Under moderate levels of Mg doping in the barrier (3–5 × 10^{18} cm^{-3}), enhancement in the output power was observed compared to LEDs with undoped barriers. The enhancement can be attributed to improved hole transport between QWs and will be further discussed in detail in this paper. However, with heavy Mg doping in the barriers (>1 × 10^{19} cm^{-3}), the output power is reduced significantly. Dual peaks in the electroluminescence (EL) spectrum were observed under low injection current (I = 5mA) for LEDs with high Mg doping (3 × 10^{19} cm^{-3}) in the middle barrier. These spectra are shown in the inset of Figure 1(a). The energy separation between the two peaks is approximately 180–200 meV, indicating that the longer wavelength transition may occur between the conduction band and the Mg acceptor level or Mg-H complexes in the QWs. At higher injection current (I = 40 mA), the transition between the conduction band and the Mg acceptor level saturates and the transition between conduction band and the valence band dominates. The drop in output power for LEDs with high Mg doping in the middle barrier is likely due to the inefficient conduction band to acceptor transition or to an increase in non-radiative recombination from the diffusion of Mg into the QWs. This suggests a trade-off between carrier transport and recombination efficiency in the QWs.

EL wavelengths under injection currents ranging from 2 mA to 100 mA were also recorded for LEDs with different Mg doping concentrations in the middle barrier. The EL peak wavelengths are plotted with the applied bias corresponding to each injection current in Figure 1(b). For each LED, increasing the injection current caused a blueshift in the EL wavelength. The blueshift can be explained by band-filling, carrier screening, or band-bending across the active region. Under the same current injection, the LEDs with higher Mg doping concentrations in the middle barrier have longer emission wavelengths and lower applied biases. However, the LEDs all have similar EL peak wavelengths under the same applied bias regardless of the different current injection levels. This suggests that the voltage across the active region dominates the wavelength shift behavior of (20$\bar{2}$1) MQW LEDs, which is consistent with previously reported results.[12] Therefore, in addition to increasing the In composition, reducing the device voltage also plays an important role in achieving longer emission wavelengths for (20$\bar{2}$1) LEDs.

To experimentally examine the influence of Mg-doped barriers on the hole transport between QWs, dichromatic DQW LEDs with undoped or Mg-doped barriers were grown on the (20$\bar{2}$1) plane. The epitaxial structure was similar to the previously discussed LEDs, but the two QWs were grown under different temperatures. The p-side QW was grown at 765 °C while the n-side QW was grown at 865 °C. The emission wavelengths for the two QWs were 515–520 nm and 410–420 nm, respectively. Figures 2(a) and 2(b) show the EL spectra for the LEDs with undoped barriers and Mg-doped barriers (~6 × 10^{18} cm^{-3}), respectively. In Figure 2(a), only a single peak in the green region was observed, which implies that most of the recombination takes place in the QW near the p-side and that the holes mostly populate the top QW under injection currents up to 100 mA. In Figure 2(b), emission in the green region dominates under low current injection. As the injection current is increased, emission in the violet region emerges and the intensity becomes comparable to that of the green emission at higher injection levels. Figure 2(a) explains the difficulty in making high brightness MQW LEDs with long wavelength emission. As the number of QWs increases, the electrons are distributed among the wells but most of the holes populate the QW closest to the p-side. This reduces the radiative efficiency of the remaining QWs. The addition of Mg doping in the middle barrier enhances hole transport between the QWs and improves the radiative efficiency of the QW closer to the n-side. Considering the trade-off between enhanced carrier transport and radiative efficiency in each QW, the overall radiative efficiency of the active region could be increased with an optimized Mg doping profile in barriers.

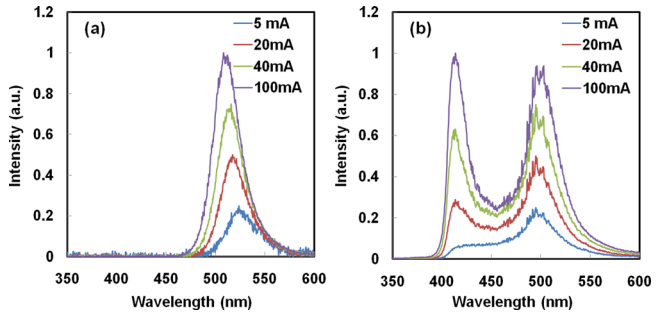

FIG. 2. (Color online) The EL spectra of dichromatic DQW LEDs with (a) undoped barriers and (b) Mg-doped barriers under various injection levels.

To examine the effects of Mg doping in barriers on the band diagram, modeling of the LED structures was carried out using the SIMULED package developed by the STR Group.[13] The potential distribution and quasi-Fermi levels were calculated by solving the Schrödinger-Poisson equations self-consistently. A drift-diffusion current model was incorporated for the simulation of the device operation under high bias voltage (3.5 V) over the p-n junction. The strain and polarization effects in semipolar InGaN were accounted for. Figures 3(a) and 3(b) show the simulated band diagrams for the (20$\bar{2}$1) DQW green LEDs with and without Mg doping in the middle barrier, respectively. Due to the inverse polarization in the QWs on the (20$\bar{2}$1) plane compared to those on the c-plane,[14] an additional energy barrier (ΔE) is present for carriers traversing the QWs. With lower effective mass and broader distribution of kinetic energy, electrons overcome the energy barrier more easily than holes. The injected holes are scattered by the additional energy barrier caused by internal polarization in the QW. The valence bands near the active region for both LEDs are plotted in Figure 3(c). Figure 3(c) shows that after Mg doping in the barrier, band-bending in the barrier creates a reduced effective barrier thickness for holes, which should enhance hole transport. Overall, the injection current and hole concentration at both QWs were both increased after Mg doping under the same bias.

We also applied the Mg doping technique to LEDs with AlGaN barriers. AlGaN barriers have been used for improving crystal quality in semipolar MQW green LDs.[15] They can be also used to increase the In composition of QWs while still maintaining high crystal quality. Combining the

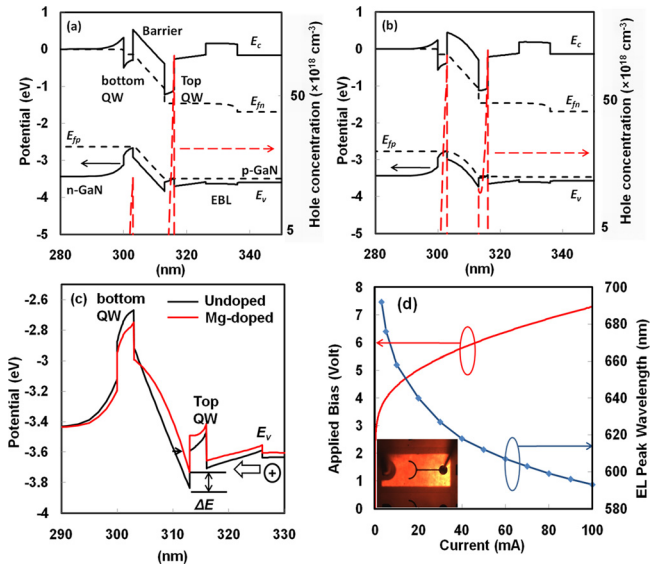

FIG. 3. (Color online) Simulated band diagrams and hole concentrations of (20$\bar{2}$1) DQW green LEDs with (a) undoped and (b) Mg-doped barriers. (c) Magnification of valence bands near the active region for both LEDs. (d) Voltage and emission peak wavelength of the orange-red LED under various injection levels. An optical micrograph under 40 mA injection is shown in the lower left corner.

Mg barrier doping and AlGaN barriers, DQW LEDs on the (20$\bar{2}$1) plane with orange-red emission were demonstrated under CW operation. Figure 3(d) shows the voltage and peak emission wavelength under various injection currents. The peak wavelength under 10 mA current injection is longer than 650 nm and it blueshifts to 590–600 nm under 100 mA injection current. The long wavelength at low injection current can be explained by reduced applied bias under low injection current with Mg doping in the middle barrier. The large blueshift with injection current is likely due to the strong quantum confinement stark effect (QCSE) caused by the large strain in QWs. The dependence of the EL wavelength on the applied voltage is similar to the result shown in Figure 1(b).

In conclusion, we have presented evidence that hole transport between QWs is a limiting factor for the performance of long wavelength LEDs on the (20$\bar{2}$1) plane. The EL wavelength is more dependent upon the applied bias across the active region than the current injection level. In a dichromatic DQW LED experiment with undoped barriers, only emission from the top QW was observed, which provides direct evidence that hole transport is poor in typical long wavelength (20$\bar{2}$1) MQW LED structures. The output power of the DQW green LED was significantly enhanced and the forward voltage was reduced with moderate Mg doping in the middle barrier. Simulations confirmed that with Mg doping in the middle barrier, the effective barrier thickness for holes between adjacent QWs is reduced due to band-bending. The simulation also suggests that the hole concentration in the QWs and the injection current are increased under the same bias with Mg doping, which is consistent with the results shown in Figure 2. These results indicate that improving hole injection efficiency is a key objective for enhancing the performance of (20$\bar{2}$1) MQW green LEDs. Additionally, we demonstrated DQW LEDs on the (20$\bar{2}$1) plane utilizing Mg doped AlGaN barriers that operate in the orange-red spectral region.

The authors acknowledge the Solid State Lighting and Energy Center at UCSB for funding. A portion of this work was done in the UCSB nanofabrication facility, part of the National Science Foundation (NSF) funded National Nanotechnology Infrastructure Network (NNIN) network. This work made use of the Central Facilities at UCSB supported by the NSF Materials Research Science and Engineering Centers (MRSEC).

[1]T. Takeuchi, H. Amano, and I. Akasaki, Jpn. J. Appl. Phys. **39**, 413 (2000).
[2]J. S. Speck and S. F. Chichibu, MRS Bull. **34**, 304 (2009).
[3]H. Ohta and K. Okamoto, MRS Bull. **34**, 324 (2009).
[4]B. Gil, P. Bigenwald, and O. Briot, Superlattices Microstruct. **44**, 291 (2008).
[5]S. H. Park and D. Ahn, Appl. Phys. Lett. **90**, 013505 (2007).
[6]Y. Zhao, J. Sonoda, C. C. Pan, S. Brinkley, I. Koslow, K. Fujito, H. Ohta, S. P. DenBaars, and S. Nakamura, Appl. Phys. Express **3**, 102101 (2010).
[7]H. Zhong, A. Tyagi, N. N. Fellows, F. Wu, R. B. Chung, M. Saito, K. Fujito, J. S. Speck, S. P. DenBaars, and S. Nakamura, Appl. Phys. Lett. **90**, 233504 (2007).
[8]S. Yamamoto, Y. Zhao, C. C. Pan, R. B. Chung, K. Fujito, J. Sonoda, S. P. DenBaars, and S. Nakamura, Appl. Phys. Express **3**, 122102 (2010).
[9]H. Sato, R. B. Chung, H. Hirasawa, N. Fellows, H. Masui, F. Wu, M. Saito, K. Fujito, J. S. Speck, S. P. DenBaars, and S. Nakamura, Appl. Phys. Lett. **92**, 221110 (2008).
[10]A. David, M. J. Grundmann, J. F. Kaeding, N. F. Gardner, T. G. Mihopoulos, and M. R. Krames Appl. Phys. Lett. **92**, 053502 (2008).
[11]S. H. Han, C. Y. Cho, S. J. Lee, T. Y. Park, T. H. Kim, S. H. Park, S. W. Kang, J. W. Kim, Y. C. Kim, and S. J. Park, Appl. Phys. Lett **96**, 051113 (2010).
[12]Y. S. Kim, A. Kaneta, M. Funato, Y. Kawakami, T. Kyono, M. Ueno, and T. Nakamura, Appl. Phys. Express **4**, 052103 (2011).
[13]V. F. Mymrin, K. A. Bulashevich, N. I. Podolskaya, I. A. Zhmakin, S. Yu. Karpov, and Yu. N. Makarov, Phys. Status Solidi C **2**, 2928 (2005).
[14]A. E. Romanov, T. J. Baker, S. Nakamura, and J. S. Speck, J. Appl. Phys. **100**, 023522 (2006).
[15]Y. D. Lin, S. Yamamoto, C. Y. Huang, C. L. Hsiung, F. Wu, K. Fujito, H. Ohta, J. S. Speck, S. P. DenBaars, and S. Nakamura. Appl. Phys. Express **3**, 082001 (2010).